Crystal Structure, Conformation, and Morphology of Solution-Spun Poly(L-lactide) Fibers

W. Hoogsteen, A. R. Postema, A. J. Pennings, and G. ten Brinke*

Department of Polymer Chemistry, University of Groningen, Nijenborgh 16, 9747 AG Groningen, The Netherlands

P. Zugenmaier

Institut für Physikalische Chemie der TU Clausthal, Arnold-Sommerfeld-Strasse 4, D-3392 Clausthal-Zellerfeld, FRG. *Received April 21, 1989; Revised Manuscript Received June 29, 1989*

ABSTRACT: Depending on the spinning and drawing conditions, two crystal structures for solution-spun poly(L-lactide) are obtained. The pseudoorthorhombic α structure (a = 10.6, b = 6.1, and c = 28.8 Å) contains two chains in the unit cell and is found at relatively low drawing temperatures and/or low hot-draw ratios. At higher drawing temperatures and/or higher hot-draw ratios a second so-called β structure appears. For this structure an orthorhombic unit cell is proposed (a = 10.31, b = 18.21, and c = 9.00 Å) containing six chains. The chain conformations of the α and β structure are left-handed 10/3 and 3/1 helices, respectively. Calculations show that both conformations have approximately the same energy. Therefore, the preference for one of the two structures is determined by packing considerations. In fibers containing a mixture of α and β structure, the latter seems to bear most of the load during stress–strain experiments. Meridional small-angle X-ray scattering experiments yield a maximum for fibers containing only α structure pointing to a lamellar folded-chain morphology. The β structure on the other hand seems to correspond to a fibrillar morphology. Differential scanning calorimetry on unconstrained fibers shows that the β structure melts at a lower temperature than the α structure. The large shift of the peak melting temperature to higher temperatures in melting experiments on constrained fibers indicates that both lamellae and fibrils contribute to the strength of the fibers. This points to a considerable amount of interconnections/entanglements between adjacent lamellae.

1. Introduction

In recent years the preparation of high-strength poly(L-lactide) (PLLA) fibers has been studied[1-8] because of its potential applications as a suture in microsurgery and in composite materials. Compared to melt-spinning, the preparation of PLLA fibers from semidilute solutions using a dry-spinning process yields fibers with improved tensile properties due to a reduction in the number of entanglements. The final properties depend in a complex way on spinning variables such as molecular weight, molecular weight distribution, solvent quality and solvent composition,[5] ambient temperature,[6] spinning speed, spinline draw ratio, and die geometry.[8] The same holds for the hot-draw variables such as drawing temperature and deformation rate.[7] With the spinning and drawing conditions optimized, PLLA fibers with a tensile strength up to 2.3 GPa and a Young's modulus of 16 GPa have been produced from solutions of PLLA in mixtures of chloroform and toluene near Θ conditions.[7]

Wide-angle X-ray scattering (WAXS) studies of PLLA fibers revealed the existence of two crystal modifications. The structure of the α crystal modification is pseudoorthorhombic with the chains in a −10/3 helical conformation as determined by De Santis and Kovacs.[9] Eling et al.[1] reported for the first time the existence of another modification, which they called the β structure. Fibers containing this β-crystal modification, but considerable α structure as well, were spun from semidilute solutions of PLLA in toluene and afterward hot-drawn to high hot-draw ratios.

In this paper the influence of the preparation conditions on the presence of the crystal modifications will be discussed in detail. A proposal for the unit cell dimensions of the β structure will be presented, and the results of conformational energy calculations for chains in both structures will be compared. Moreover, the influence of the two modifications on the ultimate fiber properties will be considered.

2. Experimental Procedures

Poly(L-lactide) was synthesized by polymerization of L-lactide using stannous 2-ethylhexanoate as a catalyst. The procedure is described in detail in ref 10. The spinning solution was prepared by dissolving PLLA in chloroform at room temperature. Subsequently, toluene was added and the solution was homogenized without mechanical stirring.[5,7] Before extrusion the PLLA solution was conditioned in a piston-cylinder apparatus at 70 °C for 3 h. The solution was extruded at 60 °C (20 °C in the case of pure chloroform) through a stainless steel, conical die (entrance angle 43°, length 23 mm, and exit diameter 0.25 mm) and collected at 20–22 °C on sand-blasted glass bobbins without applying additional stress to the extrudate. The spinning speed varied from 1 to 7 m/min.[5,7] The hot-drawing experiments were carried out in a heated double-walled glass tube (length 0.6 m) at different temperatures and different entrance velocities (0.25–6.3 cm/min) in a nitrogen atmosphere.

For the scattering experiments (WAXS/SAXS) Cu Kα radiation (λ = 0.154 nm) was used, produced by a Philips X-ray generator connected to a closed cooling circuit and operated at 45 kV and 45 mA. Small-angle X-ray scattering (SAXS) experiments were carried out using a Kratky camera equipped with a proportional counter and an electronic step scanner. Monochromatization was achieved by using a Ni filter and pulse height discrimination. The entrance slit was 80 μm. Samples for meridional experiments were prepared by winding a fiber on a rectangular frame over a length that corresponds to the length of the slit. In this way many cross sections are irradiated. It should be noticed that in this way two layers of fibers are obtained, slightly displaced by the frame thickness, and that the fibers are inclined a little with respect to the vertical as a result of the pitch. WAXS measurements were carried out using a Statton camera (pinhole collimation).

0024-9297/90/2223-0634$02.50/0

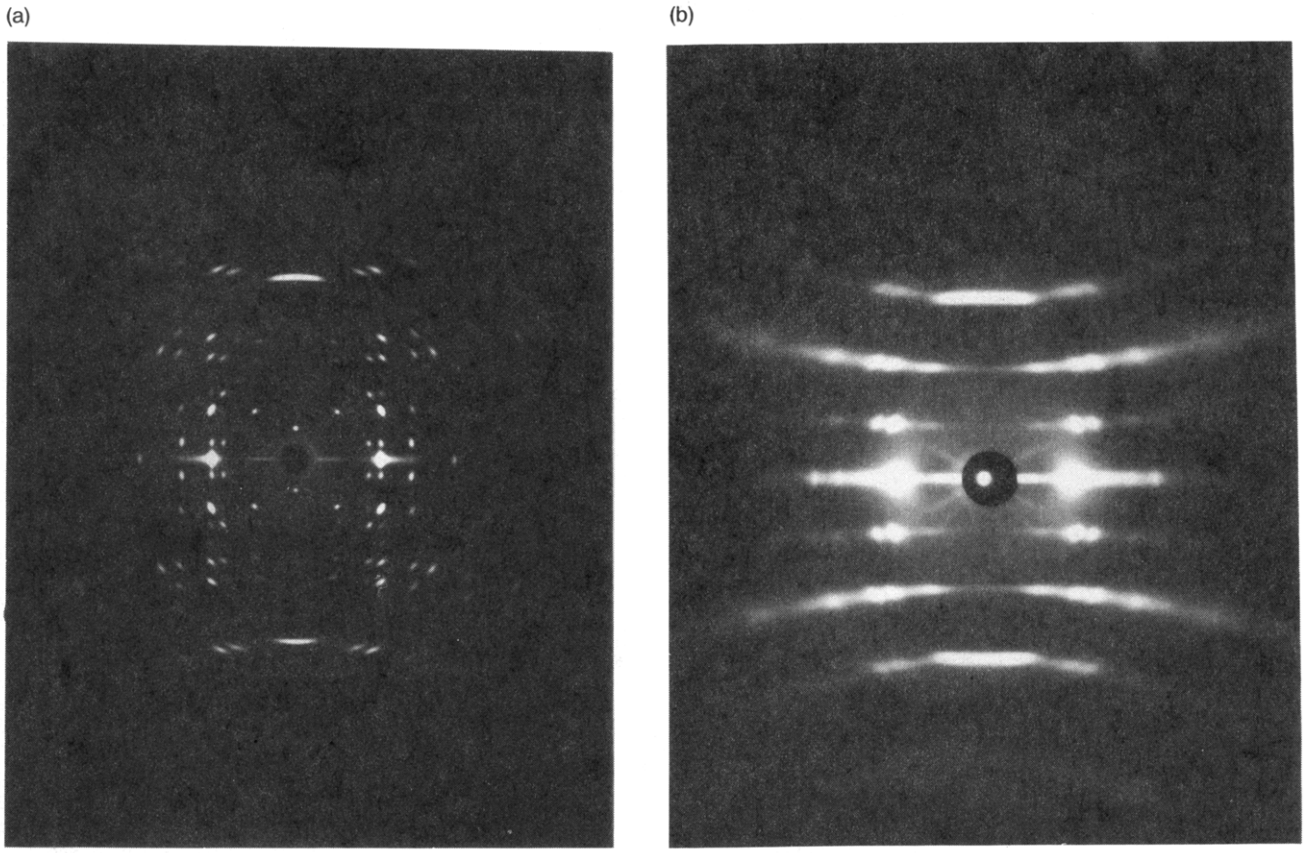

Figure 1. WAXS patterns of a fiber containing (a) only α structure (−10/3 helix) and (b) only β structure (−3/1 helix).

Real-time WAXS experiments on fibers during straining at room temperature were carried out at the synchrotron of DESY (Hamburg). A one-dimensional position-sensitive detector was used to record the intensity. Bundles of six fibers were drawn with a speed of 0.55 cm/min. The starting length of the specimens was 80 mm. The melting behavior of the fibers was investigated with a Perkin-Elmer DSC7 differential scanning calorimeter. Sample sizes were between 0.4 and 1.5 mg, and scans were taken from 373 to 523 K. For melting experiments on unconstrained fibers, the fibers were cut into small pieces of ca. 3 mm in length. In the case of melting experiments on constrained fibers, the fibers were tightly wound around a small aluminum frame with dimensions of 4 × 4 mm^2. The ends of the fibers were fixed to the frame. To provide good thermal contact between sample and sample pan, a droplet of silicone oil was added. The reference sample pan was equipped with a droplet of silicone oil as well, and in the case of "constrained" melting also with an aluminum frame.

3. Results and Discussion

3.1. Fiber Preparation. In order to determine the unit cell dimensions of the β-crystal modification of PLLA, attempts were made to prepare fibers containing this modification only. This turned out to be a complicated problem. The amount of β structure depends on the hot-drawing variables; the ratio β/α increases with increasing hot-draw ratio. At low hot-draw ratios only α structure is obtained. High hot-draw ratios yield a wide range of β/α ratios depending on the drawing temperature, for example, higher drawing temperatures leading to higher β/α ratios. Hot-drawing at temperatures above 200 °C could only be carried out at relatively high entrance velocities because at lower velocities fiber fracture occurs due to insufficient orientation during drawing as a result of a higher chain mobility at these temperatures.[7] Moreover, there is a tendency for the degree of β structure to decrease with increasing entrance velocity at a fixed drawing temperature. In addition to the drawing variables, the β/α ratio also depends on the spinning variables. A very important one turned out to be the molecular weight and the molecular weight distribution. Leenslag et al.[5] showed that a fiber spun from a solution of 4 wt % PLLA (M_v = 9 × 10^5 kg/kmol) in a mixture of 40/60 (v/v) chloroform/toluene and afterward hot-drawn at 204 °C to a hot-draw ratio 20 contained only β structure. After fractionation the molecular weight of this PLLA sample increased to M_v = 1 × 10^6 kg/kmol. Spinning and drawing this PLLA sample in the same way as described above led to a reduction of the maximum hot-draw ratio to 13 and a mixture of α and β structure. However, these experiments were difficult to reproduce; a subsequent attempt with a PLLA sample with M_v = 9.1 × 10^5 kg/kmol resulted in a maximum hot-draw ratio of 12 only and a mixture of a lot of β structure and some α structure. A possible reason could be a slight difference in molecular weight distribution of the two PLLA samples. Attempts to prepare fibers containing only β structure from PLLA samples with a lower molecular weight (M_v = 5.6 × 10^5 kg/kmol) were more successful. For instance, a PLLA fiber spun from a solution of 8 wt % PLLA in chloroform and afterward drawn at a temperature of 204 °C (entrance velocity 6.3 cm/min) resulted in a pure β structure for hot-draw ratios between 14 and 19. It should be mentioned that all the pure β-containing fibers are prepared under drawing conditions leading to inhomogeneous drawing.[7]

3.2. Wide-Angle X-ray Scattering. In parts a and b of Figure 1 the wide-angle X-ray scattering patterns of, respectively, the α and β structure of PLLA are presented (incident X-ray beam perpendicular to the fiber axis; fiber axis vertical). The β structure is characterized by a −3/1 helical conformation with a fiber repeat

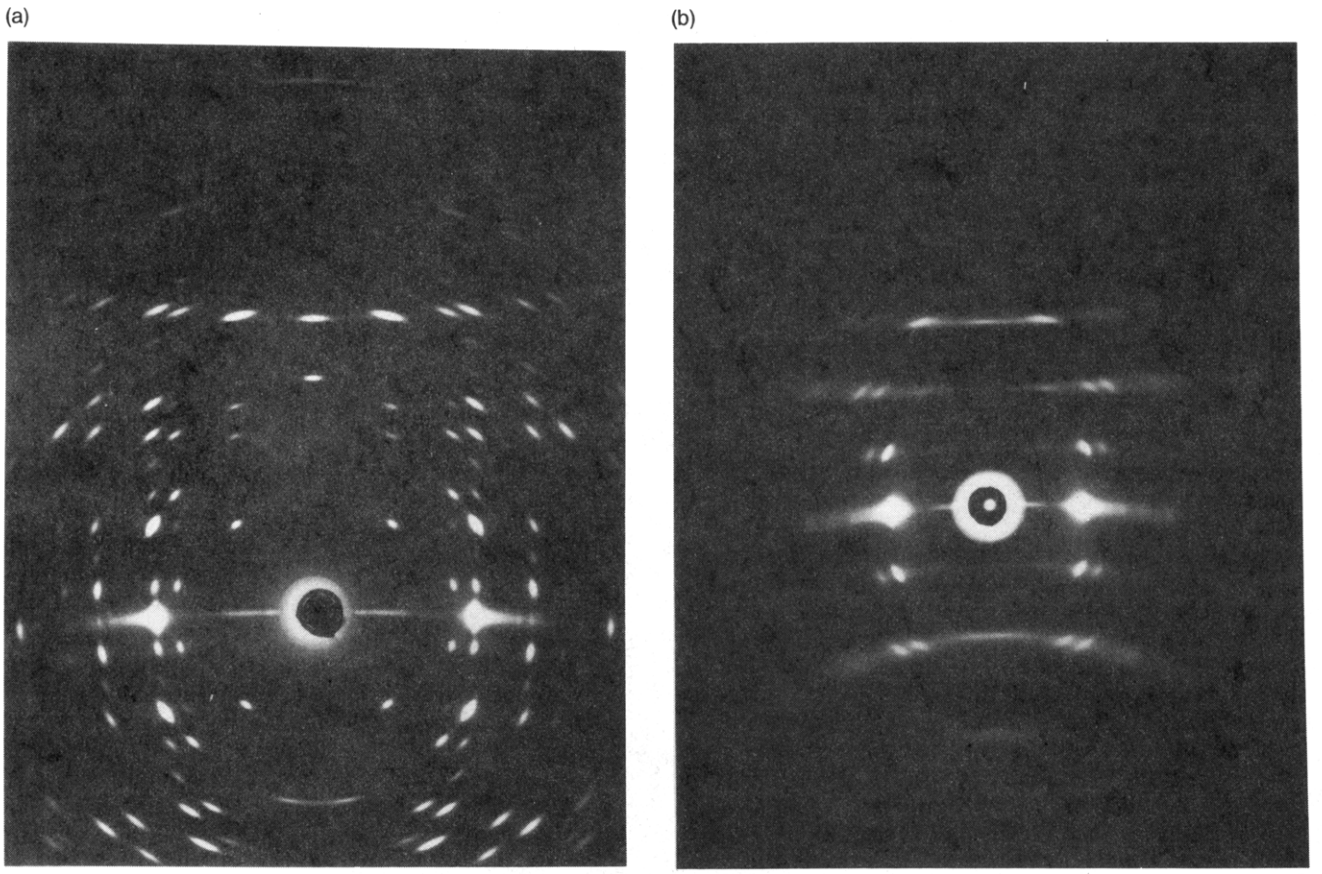

Figure 2. WAXS patterns of tilted fibers showing the meridional reflections of (a) α structure (−10/3 helix, tilt ≈15°; notice the larger scale) and (b) β structure (−3/1 helix, tilt ≈ 15°).

of 9.0 Å, which corresponds to an arise per monomeric residue of 3.0 Å. The α structure can be described best as a −10/3 helical conformation with a fiber repeat of 28.8 Å. (The unit cell axes calculated by us differ slightly from the values obtained by De Santis et al.,[9] i.e., a = 10.6, b = 6.1, and c = 28.8 Å.) The presence of meridional reflections on the second, fourth, sixth, seventh, eighth, and ninth layer line, already observed by De Santis et al.,[9] argue against a pure −10/3 helical conformation of the chains. However, the layer-line intensities support the idea that only a small deviation of a −10/3 helix occurs. The meridional reflections on the even layer lines are relatively strong compared to those on the odd layer lines (Figure 2a; tilt ≈ 15°). The suggestion of the above-mentioned authors that a coiled coil structure of the −10/3 helix is responsible for the presence of these additional meridional reflections is not very likely. Coiled coil structures[11-15] can account for the presence of an extra meridional reflection at d = 5.15 Å in α-keratin, which has a layer-line structure slightly displaced from that of a straight polypeptide α helix (18/5). However, meridional reflections are observed in many other synthetic polymers. For instance, the α-helix structure of poly(L-alanine),[16-19] the polypeptide "analogon" of PLLA, shows two extra meridional reflections. These reflections were ascribed to a periodic distortion of the nonintegral 47/13 helix as a result of a close packing of the chains in the hexagonal unit cell, which is governed by the interchain contacts between the methyl groups. Probably the packing of the PLLA chains in the (nearly) hexagonal α structure leads to a distortion of the pure −10/3 helical conformation in a similar way. Other examples of diffraction patterns containing unexpected meridional reflections are obtained for several homopolypeptides (α helixes),[19] poly(oxymethylene),[20,21] and amylose triacetate II.[22]

Figure 2b shows the X-ray pattern of a tilted β structure containing fiber (tilt ≈ 15°). The observed 0,0,3 reflection indicates that the chain conformation of the β structure is indeed a pure −3/1 helix (no unexpected meridional reflections could be detected). Striking are the streaks on the layer lines (except the equator), which point to a certain degree of disorder in the mutual level of the chains in the fiber axis direction. This type of disorder is also found for several other aliphatic polyesters such as poly(ϵ-caprolactone)[23] and, in a very extreme way, for poly(β-propiolactone).[24] In the latter case only continuous scattering on each layer line (except the equator) is observed.

The reflections for the β structure of PLLA can be indexed with an orthorhombic unit cell, containing six chains and axis a = 10.31, b = 18.21, and c = 9.00 Å. The calculated and observed d spacings are collected in Table I. Relatively large differences between calculated and observed values are found for the 111 and 112 reflections as compared to all the other reflections. These reflections are extremely broad in the direction along the layer lines, and their exact values are hard to determine. The proposed unit cell for the β structure has a base-plane dimension very close to 3 times the base plane of the α structure ($a_\alpha \approx a_\beta$, $b_\beta \approx 3b_\alpha$). In fact, a close resemblance may be expected since the change of a −10/3 to −3/1 helical chain conformation results only in a small increase of the rise per monomeric residue from 2.88 to 3.0 Å. Unit cells containing six chains are somewhat unusual but have been proposed before for cellulose and amylose derivates.[22,25,26]

3.3. Conformation. Calculation of the most stable conformation of an isolated polymer chain can be very useful for the determination of the crystalline structure of polymers since, as shown by De Santis et al.,[27] in many cases the helical conformation found in semicrystalline

Table I
Calculated and Observed d Spacings (Å) of the β Structure of Poly(L-lactide) with the Orthorhombic Unit Cell a = 10.3, b = 18.2, and c = 9.0 Å

h,k,l	$d_{h,k,l}$(calc)	$d_{h,k,l}$(obs)	intens
200	5.16	5.17	vs
240	3.41	3.40	m
330	2.99	3.00	m
070	2.60	2.60	w
350	2.50	2.50	w
460	1.97	1.96	w
111	6.35	6.20	w
131	4.52	4.53	s
221	4.02	4.02	s
311	3.16	3.17	m
251	2.83	2.82	m
351	2.41	2.42	w
112	4.02	3.98	m
132	3.41	3.42	s
222	3.18	3.17	m
312	2.70	2.70	w
422	2.17	2.17	w
003	3.00	3.00	m
023	2.85	2.86	s
133	2.60	2.61	m
043	2.51	2.50	m
243	2.25	2.25	w
253	2.11	2.11	w
073	1.97	1.97	w

Table II
Discrete Energy Minima for PLLA Chains According to the Conformational Energy Calculations of Flory and Co-workers[33]

	ψ	Φ, deg	E, kcal/mol	state[a]
I	130	110	0.08	$g^+_\psi g^+_\Phi$
II	130	20	1.40	$g^+_\psi t_\Phi$
III	−20	110	0	$t_\psi g^+_\Phi$
IV	−20	20	1.52	$t_\psi t_\Phi$

[a] t = trans; g = gauche.

materials is determined largely by the intramolecular interactions. In other cases the packing, i.e., intermolecular interactions, may influence the conformation of the chains in the crystal considerably. The latter is the case for polypeptides.[28-31] For example the β-pleated sheat (nearly extended) polypeptide crystal structure is stabilized by interchain hydrogen bonds.

Flory and co-workers[32,33] calculated the energetic most stable conformations for PLLA chains. In these calculations trans planarity of the ester group was assumed on the basis of microwave spectroscopy, electron diffraction, and infrared experiments on various esters.[34-37] According to Cornibert et al.[38] deviations greater than 10° from trans planarity are unlikely for low molecular weight ester groups. They calculated that the minimum chain conformational energy of poly(pivalolactone) corresponds to trans planarity using a potential barrier for the rotation around the carbonyl carbon/ester oxygen of 8.75 kcal/mol.[39] Similar results were obtained for some other poly(β-hydroxyalkanoates).[40,41] On the other hand, relatively large deviations from trans planarity were found for poly(ethylene adipate) and poly(ethylene suberate).[42]

The calculations of the conformation for PLLA chains by Flory and co-workers yielded four discrete energy minima, I–IV (Table II), corresponding approximately to the conventional trans (t) and gauche (g^+) states for ψ and Φ (Figure 3). State I corresponds to the most compact chain conformation, and IV is the most extended conformation. The conformations with Φ in the nearly trans conformation (II and IV) are energetically less favorable than the gauche conformations (I and III). On the other hand, the nearly trans and gauche conformations of ψ are energetically comparable. Previous calculations of the conformation of PLLA by De Santis and Kovacs[9] yielded only two discrete energy minima at ψ = −30°, Φ = 115°, and ψ = 150°, Φ = 115°, which are very close to the low-energy minima I and III. They showed that the conformation of the chains in the α crystal structure is only compatible with minimum III. This implies that the −10/3 helix is left-handed (this in contrast to I, which is only compatible with a right-handed helix with helical parameters very close to the characteristic R_α helix for polypeptides).

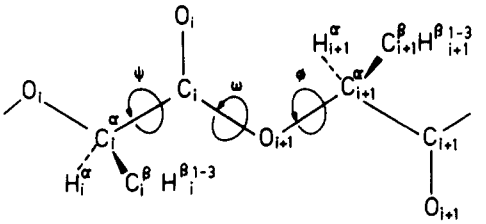

Figure 3. Schematic representation of a part of the PLLA chain (residue i and i + 1) with the atom numbering and the determination of the angles as used in this paper (ψ = 0°, trans; Φ = 0°, trans).

Table III
Standard Bond Lengths and Bond Angles Used in the Conformational Energy Calculations (Taken from De Santis et al.[9])

bond	length, Å	bond	angle, deg
O(ester)–C_α	1.46	$O_eC_\alpha C_c$	109.5
C_α–C(carbonyl)	1.53	$C_\alpha C_eO_e$	110
C(carbonyl)–O(ester)	1.31	$C_cO_eC_\alpha$	118
C(carbonyl)–O(carbonyl)	1.19	$O_cC_cO_e$	125
C_α–C_β	1.52	$O_eC_\alpha H_\alpha$	109.5
C_α–H_α	1.05	$O_eC_\alpha C_\beta$	109.5
C_β–H_β	1.05	$C_\alpha C_\beta H_\beta$	109.5

A calculation of the conformation of a PLLA −10/3 helix and a −3/1 helix (β structure) may give information about the relative stability of the two crystal modifications although the molecular packing can also play an important role. These conformations were calculated using the computer program developed by Zugenmaier and Sarko[43,44] for the conformational and packing analyses of polysaccharides. With this program the conformation and packing can be refined simultaneously by the variable virtual bond method. In the refinement of the conformation the bond lengths, bond angles, and conformation angles are optimized with respect to a set of standard values by minimizing the bonded and nonbonded interactions (Lennard-Jones potentials). For the standard bond lengths and bond angles the values according to De Santis et al.[9] were used (Table III). The different atoms, bond lengths, and conformation angles are defined in Figure 3. Trans planarity was assumed for the ester group (ω = 0°).

The calculation of the conformation of the −10/3 helix yielded a minimum for ψ = −30° and Φ = 115°. These values are the same as obtained by De Santis et al.[9] The values found for the −3/1 helix were ψ = −36° and Φ = 106°, very close to the values of the −10/3 helix. This close similarity could be expected since the −3/1 helix is only slightly more extended than the −10/3 helix (rise per monomeric residue 3.0 and 2.88 Å, respectively). The values for the nonbonding and bonding interactions were comparable for both structures. The conformation angles of both helices are located in the range corresponding to the energy minimum III. The energy minimum IV found by Flory and co-workers[33] is far off the region of the con-

Table IV
Cartesian Coordinates (Å) of the Atoms of the Basic Residue of the α Structure of PLLA (Ester Oxygen Placed on the y Axis)

atom	x, Å	y, Å	z, Å
O(ester)	0.000	−1.237	0.000
C_α	−0.921	−1.099	1.118
C(carbonyl)	−0.259	−0.292	2.232
O(carbonyl)	0.910	−0.245	2.458
C_β	−1.287	−2.475	1.647
H_α	−1.790	−0.604	0.797
$H_{\beta,1}$	−2.141	−2.828	1.149
$H_{\beta,2}$	−0.489	−3.137	1.485
$H_{\beta,3}$	−1.485	−2.412	2.676

Table V
Cartesian Coordinates (Å) of the Atoms of the Basic Residue of the β Structure of PLLA (Ester Oxygen Placed on the y Axis)

atom	x, Å	y, Å	z, Å
O(ester)	0.000	−1.039	0.000
C_α	−0.884	−0.903	1.155
C(carbonyl)	−0.112	−0.274	2.318
O(carbonyl)	1.023	−0.506	2.593
C_β	−1.389	−2.275	1.569
H_α	−1.699	−0.290	0.903
$H_{\beta,1}$	−1.987	−2.674	0.803
$H_{\beta,2}$	−0.572	−2.911	1.741
$H_{\beta,3}$	−1.957	−2.190	2.449

formation angles ψ and Φ obtained for the −3/1 helix. This minimum IV corresponds to even more extended helices such as (nearly planar) 2/1 helices, which occur for many other aliphatic polyesters.[45] Therefore, the packing of the chains must be the most important factor responsible for the appearance of the two crystal modifications.

No attempts to calculate the packing of these crystal structures were made. Especially for the β structure, containing six chains in the unit cell, a calculation will be very difficult and time consuming. The atomic coordinates of one monomeric residue for the α and β structure each are presented in Tables IV and V. Figures 4 and 5 show the −10/3 and −3/1 helical projections, respectively, along the helical axis (*xz* plane) and perpendicular to the helical axis (*xy* plane). From these two figures it is clear that the methyl groups will contribute considerably to the interchain van der Waals interactions in the crystallites because they are located at positions farthest from the helical axis. The projections of a −10/3 helix and a −3/1 helix onto the *xy* plane (Figure 5) look somewhat different. The cross section of a −10/3 helix looks almost circular, whereas that of a −3/1 helix shows a 3-fold groove along the helical axis, into which methyl groups of neighboring chains may move to some extent with a translational degree of freedom along the helical axis. As a result a different size and symmetry of the unit cell will be obtained as well as some disorder along the helical axis, being reflected in streaks of the X-ray pattern. The −10/3 helix contains grooves also, but they are twisted around the helical axis. Similar structures were observed for polypeptide R_α helices.[12,19] Packing of these helix types in the hexagonal closest packing may lead to some degree of distortion from the pure helical conformation, which may account for extra meridional reflections often observed for these type of structures.[12,19] Moreover, a −10/3 helix with twisted grooves may restrict the translation of neighboring chains with respect to each other by a kind of interlocking of the methyl groups leading to sharp reflections on the layer lines (Figures 1a and 2a).

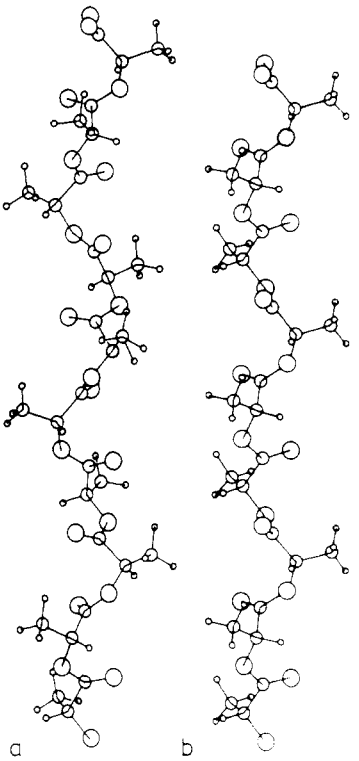

Figure 4. Projections along the helical axis of a −10/3 helical conformation (a) and a −3/1 helical conformation (b).

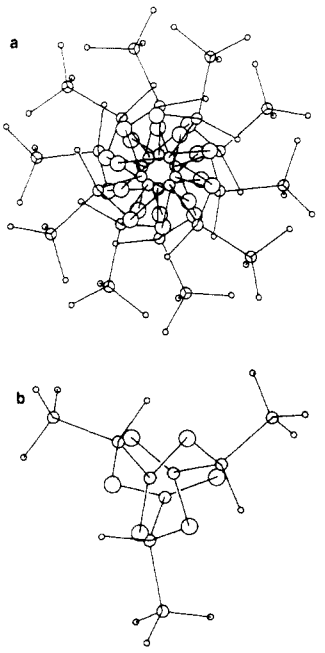

Figure 5. Projections perpendicular to the helical axis of a −10/3 helical conformation (a) and a −3/1 helical conformation (b).

In Table VI the closest nonbonding intramolecular contacts within the helix are presented. Only small differences are observed between the −10/3 and −3/1 helical conformation. The interaction between the carbonyl oxygen of residue *i* and the α carbon of the next residue gives a relatively large contribution to the nonbonding energy (distance, respectively, 2.70 and 2.69 Å for the −10/3 and −3/1 helix). Two other important contributions to the nonbonding energy arise from the small distance between O_i(ester)/O_i(carbonyl) and H_i^α/O_{i+1}(ester) resulting from the nearly trans character of the conformation angle ψ (ψ_α = −30° and ψ_β = −36° of

Table VI
Some Nonbonding Intramolecular Contact Distances r for the α and β Chain Conformations of PLLA

	r_α, Å	r_β, Å
$C_i^\beta \cdots O_i$(carbonyl)	3.23	3.16
C_i(carbonyl)$\cdots O_{i+1}$(carbonyl)	3.16	3.40
O_i(carbonyl)$\cdots C_{i+1}^\alpha$	2.70	2.69
O_i(carbonyl)$\cdots C_{i+1}$(carbonyl)	2.93	3.07
$C_i^\beta \cdots O_{i+1}$(ester)	3.11	3.11
O_i(ester)$\cdots O_i$(carbonyl)	2.80	2.84
O_i(carbonyl)$\cdots O_{i+1}$(carbonyl)	3.26	3.59
C_i(carbonyl)$\cdots C_{i+1}$(carbonyl)	2.95	3.04
C_i(carbonyl)$\cdots H_i^{\beta,3}$	2.49	2.66
C_i(carbonyl)$\cdots H_{i+1}^\alpha$	2.63	2.57
O_i(ester)$\cdots H_i^{\beta,2}$	2.46	2.70
O_i(ester)$\cdots H_i^{\beta,1}$	2.90	2.62
O_i(carbonyl)$\cdots H_{i+1}^\alpha$	2.63	2.53
$H_i^{\beta,3} \cdots O_{i+1}$(ester)	2.82	2.96
$H_i^\alpha \cdots O_{i+1}$(ester)	2.39	2.39

the α and β chain structure, respectively). All these short intramolecular contacts are so-called 1–4 contacts, which will be omitted if torsion potentials are used in the potential energy minimization procedure.

3.4. Solid-State Phase Transition. The stress–strain curves of PLLA fibers show some typical features. Fibers drawn to low hot-draw ratios show a sharp inflection/yield point at a strain of about 1–2%.[1,2] For higher hot-draw ratios this yield point is less pronounced. Relatively strong fibers (>1 GPa) yield a sigmoidal stress–strain curve with an increase of the modulus just prior to fracture.[7] The strain at break of the hot-drawn fibers varies between 10 and 35%. It is suggested that the inflection at 1–2% strain might be the result of a transition of the α to β structure.[2] Solid-state phase transitions during cold-drawing have been observed for a number of polyesters (2/1 helix to planar zigzag) such as poly(tetramethylene terephthalate) (4GT)[46] and various poly(β-hydroxyalkanoates).[45,47-49]

Real-time WAXS measurements were performed during stress–strain experiments to investigate the possibility of a phase transition of the α to β structure for PLLA during cold-drawing. To obtain enough intensity (the fiber was drawn to breakage within 2 min), the high X-ray intensity of a synchrotron source was utilized in combination with a one-dimensional position-sensitive detector. The detector was focused on the meridian around the 1,0,10 reflection of the α structure ($2\Theta = 34.24°$, d = 2.776 Å) and the high-intensity streak of the third layer line of the β structure ($2\Theta = 30.84°$, d = 2.899 Å). The starting fiber (hot-draw ratio $\lambda = 5$) contained almost only α structure, and its stress–strain curve showed a clear yield point. No transformation of the α structure into the β structure could be observed for this fiber during cold-drawing. Only an increasing shift of the 1,0,10 reflection to smaller angles together with peak broadening occurred. Another fiber, containing a mixture of α and β structure ($\lambda = 8.1$; the corresponding stress–strain curve showed only a gradually inflection) also yielded no phase transition during cold-drawing, but the reflection shifted again to smaller angles. A remarkable feature is the relatively large shift of the β reflection with regard to the shift of the 1,0,10 reflection of the α structure as shown in Figure 6. Moreover peak broadening occurred for the higher cold-draw ratios. The shift for the highest cold-draw ratio for the β streak of the third layer line is 1.47° and 0.63° for the 1,0,10 reflection. This corresponds to an increase of the c-axis of the β and α structure of, respectively, 5.2% and 2.1%, assuming that only the c dimension of the crystal changes. From this elongation of the c dimensions we conclude that the β structure carries most of the load during stress–strain experiments. Since no phase transition is observed, the characteristic shape of the stress–strain curves probably results from morphological changes such as a transformation of a lamellar structure into a more fibrillar structure. Fibers drawn to higher hot-draw ratios contain more fibrillar structures leading to a less pronounced yield point. Important information about the morphology of the hot-drawn fibers can be obtained from differential scanning calorimetry (DSC) and small-angle X-ray scattering (SAXS).

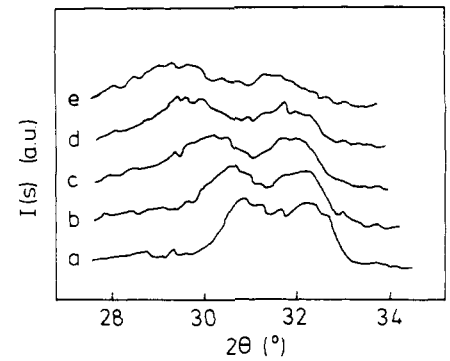

Figure 6. WAXS real-time intensity along the meridian around the third and tenth layer line of, respectively, the β and α structure for a fiber during cold-drawing to break as a function of the cold-draw ratio, ϵ. The fiber was spun from a solvent mixture of 5 wt % PLLA ($M_v = 9 \times 10^5$ kg/kmol) in 75/25 (v/v) chloroform/toluene (die diameter 1 mm) and afterward drawn to a hot-draw ratio 8.1 at a temperature of 203 °C: (a) ϵ = 0%, (b) ϵ = 1.7%, (c) ϵ = 4.0%, (d) ϵ = 6.2%, (e) ϵ = 8.5%.

3.5. Small-Angle X-ray Scattering. Small-angle X-ray scattering gives information about the presence of lamellar material in oriented fibers. In the case of gel-spun polyethylene fibers, hot-drawing of unoriented fibers to low hot-draw ratios yields a shish-kebab-like structure of fibrillar (extended chain) backbones and closely packed lamellar overgrowth oriented with the c-axis parallel to the fiber axis.[50,51] Drawing to higher hot-draw ratios leads to a higher fraction of fibrillar material and less lamellar overgrowth. SAXS experiments reveal a meridional maximum at an angle that corresponds to a period in the order of 50 nm. The intensity of this maximum decreases with increasing hot-draw ratio, but its position is hardly affected. The maximum corresponds to packing of lamellae oriented with the c-axis parallel to the fiber axis.

In Figure 7, some silt-smeared meridional scattering curves for PLLA fibers are presented. Figure 7, curve a is for a fiber drawn to a hot-draw ratio $\lambda = 4$ and contains α structure only. This curve contains a maximum at $s = 0.0186$ nm^{-1}, which corresponds to a period of 54 nm. The maximum disappears completely after drawing the same as-spun fiber to $\lambda = 8$ (Figure 7, curve b), which is still far below the maximum hot-draw ratio of 15. WAXS showed that this fiber contains a mixture of α and β structure. In addition, the intensity curve of a fiber originally prepared from another solvent mixture and drawn to a hot-draw ratio $\lambda = 12$ ($\lambda_{max} = 20$) and containing only α structure shows a faint shoulder at very small angles (Figure 7, curve c). Although hot-drawn PLLA fibers have not been studied systematically by SAXS yet, the above results indicate that a distortion of the regular packed lamellar structures is accompanied by the introduction of β structure. Since β structure is always obtained at the higher hot-draw ratios, we conclude that this structure corresponds to fibrillar (extended-chain) crystals.

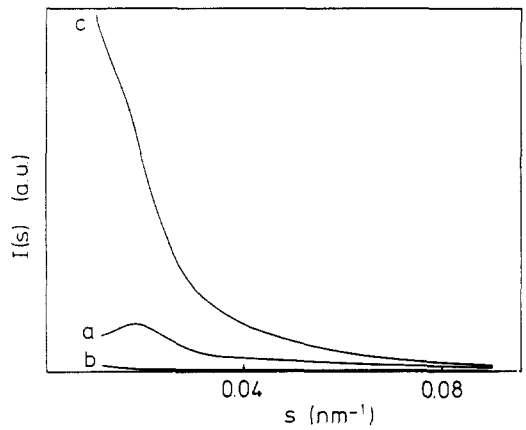

Figure 7. Slit-smeared meridional SAXS intensity curves of hot-drawn PLLA fibers prepared at different spinning conditions: (a) fiber spun from a solvent mixture of 4.5 wt % PLLA ($M_v = 9 \times 10^5$ kg/kmol) in 40/60 (v/v) chloroform/toluene and afterward hot-drawn to a draw rato $\lambda = 4$ at a drawing temperature of 191 °C (α structure); (b) same as (a), $\lambda = 8$ (mixture of α and β structure); (c) fiber spun from a solvent mixture of 4.0 wt % PLLA ($M_v = 9.1 \times 10^5$ kg/kmol) in 50/50 (v/v) chloroform/4-cymene and afterward drawn to a hot-draw ratio $\lambda = 12$ at a drawing temperature of 190 °C (α structure).

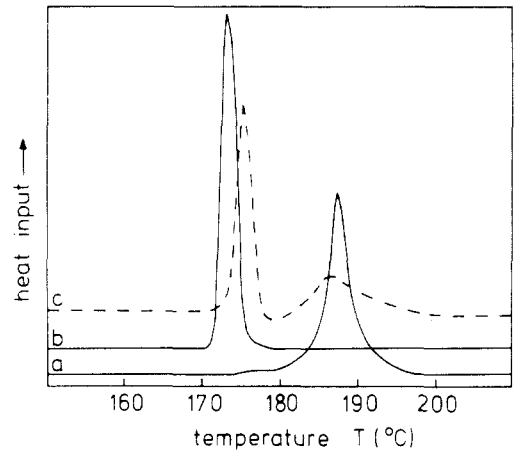

Figure 8. Thermograms showing the melting behavior of unconstrained PLLA fibers; (a) same fibers as shown in Figure 7a (only α structure); (b) fiber spun from a 8.0 wt % PLLA ($M_v = 5.6 \times 10^5$ kg/kmol) solution in chloroform and afterward hot-drawn to a ratio $\lambda = 14$ at a drawing temperature of 204 °C (only β structure); (c) fiber spun from a solvent mixture of 4.0 wt % PLLA ($M_v = 9 \times 10^5$ kg/kmol) in 40/60 (v/v) chloroform/toluene and afterward hot-drawn to a draw ratio $\lambda = 8$ at a drawing temperature of 204 °C (mixture of α and β structure).

3.6. Differential Scanning Calorimetry. As in our previous work on gel-spun polyethylene fibers[52,53] DSC experiments on hot-drawn PLLA fibers were performed for unconstrained and constrained fibers. In the first case the fibers were cut into small pieces (≈3 mm), and in the latter case the fibers were wound on an aluminum frame. In the case of polyethylene the DSC experiments on constrained fibers allowed us to distinguish between lamellar and fibrillar material because the lamellar material melted at the same temperature as in the unconstrained samples whereas the fibrillar material showed an orthorhombic to hexagonal phase transition at a much higher temperature.

In Figure 8 the endotherms for three different unconstrained PLLA fibers are presented. Curves a–c belong to fibers containing only α, only β, and a mixture of α and β structure, respectively. The β structure melts at a temperature of about 175 °C, about 10 °C below the melting temperature of the α structure (≈185 °C). From

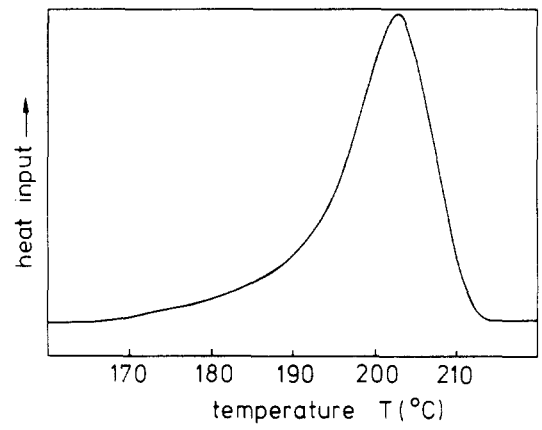

Figure 9. Thermogram showing the melting behavior of a constrained lamellae containing PLLA fiber (only α structure; same fiber as shown in Figure 7a and 8a).

this observation we conclude that the β structure is somewhat less stable than the α structure. WAXS supports this statement since, as pointed out before, the streaks of the layer lines correspond to a certain degree of disorder in the crystals. Probably the chains are forced into a somewhat less favorable packing by the high stresses during drawing, which prevents the more or less stretched chains to crystallize in folded-chain crystals. No transition of the β structure into the α structure was observed, even for a low scanning speed (1 °C/min). The melting enthalpy does not change much with the hot-draw ratio, and maximum values of about 60–65 J/g are obtained. Probably the increase of the crystallinity, which whould be expected for a transformation of lamellae into fibrillar crystals, is compensated by a lower ΔH value for the β structure.

DSC measurements on constrained fibers show broad melting endotherms. Peak melting temperatures are found in a very wide temperature range with poor reproducibility. In all cases a very large shift of the peak melting temperature to higher temperatures is observed, up to 230 °C, which had been noticed before by Eling et al.[1] Even for the fiber hot-drawn to a ratio $\lambda = 4$ and containing a lamellar structure (only α phase), a melting temperature around 200 °C (Figure 9) is found. This is in complete contrast to the results of DSC experiments on constrained gel-spun polyethylene fibers, which showed no shift of the peak melting temperature of lamellar material to higher temperatures.[52,53] Obviously, in the case of PLLA the lamellar structure is kept under considerable stress, which prevents melting. This may point to a relatively high degree of entanglements in the amorphous regions between adjacent lamellae probably as a result of the fiber preparation. Although the PLLA fibers are spun from a semidilute solution, evaporation of the solvent(s) during spinning in combination with phase separation and a relatively low crystallization rate may lead to a morphology with a lot of interconnections between adjacent lamellae. This is in contrast to the gel-spun polyethylene fibers where paraffin oil is used as a solvent. The low-maximum hot-draw ratios of PLLA (up to about 20) compared to gel-spun polyethylene ($\lambda_{max} \approx 100$) support this idea. The lack of reproducibility of the peak melting temperatures in the experiments on constrained fibers is the result of the uncontrolled stress during heating/melting, which depends for example on the way of winding the fiber onto the frame. Moreover, the fiber will melt instantaneously after fiber breakage, which occurs for the higher hot-draw ratios as can be seen from examining the sample used in the DSC experiment afterward.

3.7. Tensile Strength. In the last few years research efforts have focused on the tensile strength of PLLA fibers.[1,2,4-8] It was found to depend in a complex way on many spinning and drawing variables. One of the most striking results was that the tensile strength as a function of the hot-drawing temperature showed two maxima, one at 180–190 °C and the other at 200–210 °C.[1,4,5] After the original PLLA sample was fractionated, the distinction between these two regions became less pronounced. WAXS of fibers drawn to the maximum hot-draw ratio at the temperature corresponding to these two maxima and the minimum in between the maxima for a PLLA sample with $M_v = 9 \times 10^5$ kg/kmol revealed that the fiber spun at the first maximum (T = 190 °C, σ = 1.7 GPA) contained only α structure. The fiber drawn at 204 °C (second maximum) contained only β structure (σ = 2.1 GPa), and the fiber drawn at T = 195 °C (minimum) contained a mixture of α and β structure (σ = 1.3 GPa).[5] The fibers prepared from the fractionated sample ($M_v = 1 \times 10^6$ kg/kmol) contained only a mixture of α and β structure for these three temperatures and yielded a maximum tensile strength of 1.65 GPa (λ_{max} = 13, T = 204 °C).[5] Recently Postema et al.[7] found that the deformation rate during hot-drawing is an important factor in the preparation of strong PLLA fibers and succeeded in preparing fiber with a tensile strength of 2.3 GPa at a drawing temperature of 191 °C using a PLLA sample with $M_v = 9.1 \times 10^5$ kg/kmol. This sample showed a strong resemblance to the fractionated sample of Leenslag et al.,[5] i.e. a low-maximum hot-draw ratio of about 13 and only one maximum in the tensile strength as a function of the hot-drawing temperature. From this it is clear that as yet there appears to be no obvious relation between the tensile strength of the fiber and the amount of α and β structure. The WAXS measurements during cold-drawing and DSC measurements on constrained fibers presented in this paper show that both structures contribute to the tensile strength of the fibers. Only their relative contribution to the tensile strength probably depends strongly on the preparation conditions. Moreover, the morphology of the starting fibers determines whether a complete transformation of the α structure into the β structure can be realized during hot-drawing. For example, in the case of the fractionated sample[5] the increase of the number of entanglements may result in a better coherence between adjacent lamellae but prevents a complete transformation of the lamellae (α structure) into a fibrillar extended-chain (β) structure.

Summary

We have shown that the possibility of preparing fibers containing only β structure strongly depends on the morphology of the as-spun fibers. A remarkable feature of this structure is the streaking of the layer lines pointing to a certain degree of disorder. The proposed orthorhombic unit cell, containing six chains, with dimensions a = 10.31, b = 18.21, and c = 9.0 Å is, as expected, closely related to the α structure since the ab plane of the β structure is nearly 3 times the ab plane of the α structure and the rise per monomeric residue is nearly the same (respectively, 2.88 and 3.0 Å). Moreover, the −10/3 and −3/1 helical conformation of the chains in the α and β structure, respectively, have approximately the same energy and the packing must therefore be the main reason for the existence of the two different crystal modifications. In spite of this close resemblance, transformations between both structures were hard to obtain. A transformation of the α structure into the β structure by cold-drawing at room temperature could not be achieved. Only hot-drawing at high temperatures and high stresses (high draw ratios) leads to this transformation. Furthermore, the β structure is stable. During melting experiments on unconstrained fibers with a scanning speed of 1 °C/min, no transition of the β structure into the α structure could be observed. From these results, in combination with the observation that meridional SAXS yields a maximum for fibers containing only α structure, we conclude that the α structure corresponds to folded-chain crystals and the β structure to fibrillar crystals. Both types of structures contribute considerably to the tensile strength as demonstrated by the increase of the c-axis of the α and β structure during cold-drawing and the results of melting experiments on constrained fibers. These findings are completely different from gel-spun polyethylene fibers where the fibrillar structure is by far the most important structure contributing to the strength. In spite of the fact that both types of fibers are prepared from semidilute solutions, PLLA fibers contain probably far more entanglements. This can also account for the relatively low maximum hot-draw ratios of PLLA. The difference is attributed to the differences between the spinning processes of PLLA and polyethylene.

Acknowledgment. This study was supported by The Netherlands Foundation of Chemical Research with financial aid from The Netherlands Organization for the Advancement of Pure Research. We thank Dr. C. Riekel and H. Seidel for their contribution to the synchrotron experiments and Dr. P. F. van Hutten, D. W. Grijpma, A. Dozeman, and A. Luiten for their contribution to this paper. W.H. acknowledges Dr. H. Steinmeier, Dipl. Chem. K. Riehl, and J. Mügge for their assistance during the crystal structure study and calculations of the conformation.

References and Notes

(1) Eling, B.; Gogolewski, S.; Pennings, A. J. *Polymer* **1982**, *23*, 1587.
(2) Gogolewski, S.; Pennings, A. J. *J. Appl. Polym. Sci.* **1983**, *28*, 1045.
(3) Hyon, S. H.; Jamshidi, K.; Ikada, Y. *Polym. Prepr. (Am. Chem. Soc., Div. Polym. Chem.)* **1983**, *24*, 6.
(4) Leenslag, J. W.; Gogolewski, S.; Pennings, A. J. *J. Appl. Polym. Sci.* **1984**, *29*, 2829.
(5) Leenslag, J. W.; Pennings, A. J. *Polymer* **1987**, *28*, 1695.
(6) Postema, A. R.; Luiten, A. H.; Pennings, A. J., submitted for publication in *Polymer*.
(7) Postema, A. R.; Pennings, A. J., accepted for publication in *J. Appl. Polym. Sci.*
(8) Postema, A. R.; Luiten, A. H.; Oostra, H.; Pennings, A. J., submitted for publication in *J. Appl. Polym. Sci.*
(9) De Santis, P.; Kovacs, A. *Biopolymers* **1968**, *6*, 299.
(10) Leenslag, J. W.; Pennings, A. J. *Makromol. Chem.* **1987**, *188*, 1809.
(11) Crick, F. H. C. *Acta Crystallogr.* **1953**, *6*, 685.
(12) Crick, F. H. C. *Acta Crystallogr.* **1953**, *6*, 689.
(13) Pauling, L.; Corey, R. B. *Nature* **1953**, *171*, 59.
(14) Fraser, R. D. B.; Macrae, T. P.; Rogers, G. E. *Nature* **1962**, *193*, 103.
(15) Nishikawa, K.; Scheraga, H. R. *Macromolecules* **1976**, *9*, 395.
(16) Brown, L.; Trotter, I. F. *Trans. Faraday Soc.* **1956**, *52*, 537.
(17) Elliott, A.; Malcolm, B. R. *Proc. R. Soc. A* **1959**, *249*, 30.
(18) Arnott, S.; Wonacott, A. J. *J. Mol. Biol.* **1966**, *21*, 371.
(19) Elliott, A. In *Poly-α-Amino Acids*; Fosman, G. D., Ed.; Marcel Dekker Inc.: New York, 1967; Chapter 1.
(20) Saruyama, Y.; Miyaji, H.; Asai, K. *J. Polym. Sci., Polym. Phys. Ed.* **1979**, *17*, 1163.
(21) Saruyama, Y.; Miyaji, H. *J. Polym. Sci., Polym. Phys. Ed.* **1985**, *23*, 1637.
(22) Zugenmaier, P.; Steinmeier, H. *Polymer* **1986**, *27*, 1601.
(23) Chatani, Y.; Okita, Y.; Tadokoro, H.; Yamashita, Y. *Polymer J.* **1970**, *1*, 555.
(24) Suehiro, K.; Chatani, Y.; Tadokoro, H. *Polym J.* **1975**, *7*, 352.

(25) Zugenmaier, P. *J. Appl. Polym. Sci., Appl. Polym. Symp.* **1983**, *37*, 223.
(26) Zugenmaier, P.; Kuppel, A. *Colloid Polym. Sci.* **1986**, *264*, 231.
(27) De Santis, P.; Giglio, E.; Liquori, A. M.; Ripamonti, A. *J. Polym. Sci., Polym. Chem. Ed.* **1963**, 1383.
(28) De Santis, P.; Giglio, E.; Liquori, A. M.; Ripamonti, A. *Nature* **1965**, *206*, 456.
(29) Liquori, A. M.; De Santis, P.; Kovacs, A.; Mazzarella, L. *Nature* **1966**, *211*, 1039.
(30) Brant, D. A.; Flory, P. J. *J. Am. Chem. Soc.* **1965**, *87*, 2792.
(31) Brant, D. A.; Miller, W. G.; Flory, P. J. *J. Mol. Biol.* **1967**, *23*, 47.
(32) Tonelli, A. E.; Flory, P. J. *Macromolecules* **1969**, *2*, 225.
(33) Brant, D. A.; Tonelli, A. E.; Flory, P. J. *Macromolecules* **1969**, *2*, 228.
(34) Curl, R. F. *J. Chem. Phys.* **1959**, *30*, 1529.
(35) O'Gorman, J. M.; Shand, W.; Schomaker, V. *J. Am. Chem. Soc.* **1950**, *72*, 4222.
(36) Riveros, J. M.; Wilson, E. B. *J. Chem. Phys.* **1967**, *46*, 4605.
(37) Miyazawa, T. *Bull. Chem. Soc. Jpn.* **1961**, *34*, 691.
(38) Cornibert, J.; Hien, N. V.; Brisse, F.; Marchessault, R. H. *Can. J. Chem.* **1974**, *52*, 3742.
(39) Yan, J. F.; Vanderkooi, G.; Scheraga, H. A. *J. Chem. Phys.* **1968**, *49*, 2713.
(40) Cornibert, J.; Marchessault, R. H. *Macromolecules* **1975**, *8*, 296.
(41) Cornibelt, J.; Marchessault, R. H. *J. Mol. Biol.* **1972**, *71*, 735.
(42) Bunn, C. W.; Turner Jones, A. *Acta Crystallogr.* **1962**, *15*, 105.
(43) Zugenmaier, P.; Sarko, A. *Biopolymers* **1976**, *15*, 2121.
(44) Zugenmaier, P.; Sarko, A. In *Fibre Diffraction Methods*; French, A. D., Gardner, K. H., Eds.; ACS Symposium Series 141; American Chemical Society: Washington, DC, 1980; p 225.
(45) Brisse, F.; Marchessault, R. H.; Perez, S. In *Preparation and Properties of Stereoregular Polymers*; Lenz, R. W., Clardelli, F., Eds.; Reidel: Dordrecht, The Netherlands, 1979; p 407.
(46) Jakeways, R.; Smith, T.; Ward, I. M.; Wilding, M. A. *J. Polym. Sci. Polym. Lett. Ed.* **1976**, *14*, 41.
(47) Cornibert, J.; Marchessault, R. H.; Allegrezza, A. E.; Lenz, R. W. *Macromolecules* **1973**, *6*, 676.
(48) Prud'homme, R. E.; Marchessault, R. H. *Macromolecules* **1974**, *7*, 541.
(49) Prud'homme, R. E.; Marchessault, R. H. *Makromol. Chem.* **1974**, *175*, 2705.
(50) Van Hutten, P. F.; Koning, C. E.; Smook, J.; Pennings, A. J. *Polymer* **1983**, *24*, 237.
(51) Hoogsteen, W.; Pennings, A. J.; ten Brinke, G., submitted for publication in *Colloid Polym. Sci.*
(52) Smook, J.; Pennings, A. J. *Colloid Polym. Sci.* **1984**, *262*, 712.
(53) Hoogsteen, W.; ten Brinke, G.; Pennings, A. J. *Colloid Polym. Sci.* **1988**, *266*, 1003.

Registry No. PLLA (SRU), 26161-42-2; PLLA (homopolymer), 33135-50-1.

Effect of Tricrecyl Phosphate Doping on the Remanent Polarization in Uniaxially Oriented Poly(vinylidene fluoride) Films

Y. Takase,* J. I. Scheinbeim, and B. A. Newman

Department of Mechanics and Materials Science, College of Engineering, Rutgers University, Piscataway, New Jersey 08854. *Received December 13, 1988; Revised Manuscript Received July 17, 1989*

ABSTRACT: Uniaxially stretched films of poly(vinylidene fluoride) were doped (1 wt %) with plasticizer, tricrecyl phosphate (TCP). This slight doping with TCP was found to enhance the amount of remanent polarization in the region of low poling fields (e.g., from 1 to 6 mC/m^2 under E_p = 60 MV/m at 20 °C) and high poling fields (e.g., from 57 to 66 mC/m^2 under E_p = 200 MV/m at 20 °C). The pyroelectric coefficient has shown that the doping enhances a quite stable (up to about 140 °C) remanent polarization after high-field poling (e.g., from 10.2 to 12.5 μC/m^2/K under E_p = 200 MV/m at 20 °C). This is suggestive of a field-induced increase in crystallinity. In addition, the switching of quasi-stable dipoles (those that randomize in the 90–140 °C range) takes place at much lower electric fields than in undoped films. The present data suggest that a small amount of dopant in the noncrystalline regions greatly enhances ferroelectric dipole switching, possibly by acting in the interfacial zone between crystalline and amorphous regions.

Introduction

Plasticized polymers, such as the poly(vinyl chloride)–tricrecyl phosphate (PVC–TCP) system, offer significant advantages in their physical properties such as toughness, flexibility, oil resistance, and nonflammability as well as high electrical resistance when compared to unplasticized polymers.

Recently, it was found in our laboratories that the addition of plasticizer to poly(vinylidene fluoride) (PVF_2) films has a significant influence on their piezoelectric and pyroelectric properties. Sen et al.[1] prepared two different types of samples to examine the effects of TCP doping. One type of sample was unoriented phase II PVF_2 film that was prepared by melt crystallization. The other type of sample was oriented phase I PVF_2 film that was obtained from the phase II film by uniaxial stretching at 54 °C. For doping, the film was immersed in TCP at elevated temperatures.

In the case of the initially unoriented phase II films, the piezoelectric and pyroelectric coefficients of the doped films showed significantly improved values compared to those of the undoped films when poled under identical conditions. The results of X-ray diffraction studies of both types of samples showed that for the doped films, the phase transformation from the nonpolar phase II crystal form to the polar phase I crystal form had taken place at much lower poling fields than for undoped films.

In the case of the uniaxially oriented phase I films, doping also led to a large increase in piezoelectric and pyroelectric response.

Although X-ray diffraction data of the doped films have suggested that some preferential positioning of the dopant at the crystallite boundaries may occur, with no evidence of diffusion of the dopant into the crystalline regions, additional studies are required to gain some understanding of the mechanisms involved.

0024-9297/90/2223-0642$02.50/0